Environmental Science Nano

PAPER

View Article Online
View Journal | View Issue

Cite this: *Environ. Sci.: Nano*, 2018, 5, 1618

Thermal transformations of manufactured nanomaterials as a proposed proxy for ageing†

S. M. Briffa, *[a] I. Lynch, [a] V. Trouillet,[b] M. Bruns,[b] D. Hapiuk[c] and E. Valsami-Jones[a]

Ageing is an important part of a manufactured nanomaterial's life cycle and can be considered as a transformation over time. It is particularly relevant to nanomaterials (NMs) because they are more reactive than their bulk counterparts and therefore are likely to undergo more significant or faster transformations with time. The conditions upon exposure of a NM to the environment, *e.g.* temperature, humidity and redox, will all individually affect ageing, as well as time. In experimental simulations, time has to be substituted by a proxy that makes timescales more realistic. Thermal ageing accelerates the normal ageing processes of NMs and thus elevated temperatures can be used to simulate prolonged ageing, allowing access to information on the long-term effects of NM ageing within a shorter time. Similar approaches are utilised in experimental simulation of protein fibrillation, for example, where processes that naturally occur over decades are accelerated to days or hours. In this work, time and temperature dependent studies were carried out on a fully characterised library of laboratory synthesised comparable polyvinylpyrrolidone (PVP) capped NMs (with core compositions of ceria, copper oxide and zinc oxide) and a commercially available uncoated cerium dioxide NM, to assess their transformations. Specifically, physical and chemical changes were studied on NMs exposed to various temperatures (25, 45, 65 and 80 °C) for a period of 4 weeks. The size, zeta potential, agglomeration/aggregation and valence state of the NMs were studied through dynamic light scattering (DLS), zeta potential, ultra-violet visible light spectroscopy (UV-VIS), transmission electron microscopy (TEM) and X-ray photoelectron spectroscopy (XPS), as a function of time. Results generally show a decrease in NM stability with increasing temperature and time. Changes in the NM size and core oxidation state were noted with increasing temperature/time. These changes varied depending on the NM core composition. Additionally the PVP capping, despite stabilising the NM dispersion, still allowed the NM core to be influenced by external factors, thus indicating likely ageing-related reduction in efficiency, though to a lesser extent than the uncapped particles. Overall the experiments recorded a complex picture of transformations as a function of time/temperature highlighting the complexity of NMs' ageing.

Received 9th August 2017,
Accepted 16th May 2018

DOI: 10.1039/c7en00738h

rsc.li/es-nano

Environmental significance

Ageing is an important part of a nanomaterial's life cycle and a nanomaterial's fate. Behaviour and toxicity may change throughout its lifetime. This paper demonstrates, for the first time, the use of thermal treatment as a proxy for ageing of nanomaterials. To date, no standardised testing of nanomaterials with respect to their evolution in time exists. After accelerated ageing, physical and chemical changes were monitored in order to better understand long term behaviour with the aim to link nanomaterial toxicity to specific parameters and properties.

1. Introduction

Ageing is an important aspect of a NM's life cycle. Most NMs react in ways that change the behaviour and properties of the particles over time.[1] During ageing several structural and chemical changes occur that are dependent on external factors, such as temperature, and factors specific to a NM, such as physicochemical properties, particularly composition and concentration. Aged NMs no longer have the same characteristics as their pristine counterparts.[2–4]

[a] *School of Geography, Earth and Environmental Sciences, University of Birmingham, B15 2TT, Birmingham, UK. E-mail: BriffaSM@bham.ac.uk*
[b] *Institute for Applied Materials and Karlsruhe Nano Micro Facility, Karlsruhe Institute of Technology, Hermann-von-Helmholtz-Platz 1, 76344 Eggenstein-Leopoldshafen, Germany*
[c] *Nanoscale Physics Research Laboratory, School of Physics and Astronomy, University of Birmingham, B15 2TT, Birmingham, UK*

† Electronic supplementary information (ESI) available. See DOI: 10.1039/c7en00738h

To date, only a few ageing studies have been carried out, with some examples highlighted below. Sarathy *et al.*[1] studied the ageing of iron core/iron oxide shell NMs in water at ambient temperature, focusing on changes in their composition, structure and reactivity. Results showed that the iron NMs became more reactive in the first 2 days of water exposure and then gradually lost reactivity over the next few hundred days.[1]

Botta *et al.*[5] investigated the evolution of physical and chemical properties during artificial ageing (in the dark or under light for 48 hours at 30 °C) of four commercial sunscreens containing titanium dioxide NMs. Results showed a significant release of colloidal residues containing titanium dioxide NMs from commercial sunscreens into an aquatic environment after artificial ageing. This raised (eco)toxicity concerns for aquatic environments and highlighted the need for appropriate risk assessments to evaluate the potential fate and indirect exposure of NMs not only during their manufacture or use but also throughout their entire life cycle.[5]

Kuchibhatla *et al.*[6] studied the influence of ageing on the properties of cerium oxide NMs. The results showed that upon ageing under ambient conditions, the concentration of Ce^{4+} initially increased to a maximum intensity after 1 day which affected the characteristic yellow colour of Ce^{4+}. This intense yellow colour faded upon ageing for 1 week, suggesting a decrease in the amount of Ce^{4+} in solution. After 3 weeks of ageing, the solution appeared pale yellow in colour indicating the further reduction of Ce^{4+} and regeneration of Ce^{3+} as confirmed by UV-VIS characterisation. The authors proposed that the UV absorption band edge in ceria NMs can be affected by particle transformations and may not always be due to pure quantum confinement effects driven by particle size changes.[6]

Mudunkotuwa *et al.*[7] studied the effect of ageing of copper (Cu) NMs by characterising and comparing fresh copper NMs, aged Cu NMs, and fresh CuO NMs that differed in their level of oxidation. The Cu (aged) NMs were generated by allowing fresh Cu NMs to sit in a laboratory environment for several years under ambient conditions. Analysis took place as a function of pH and in the presence and absence of citric and oxalic acid. The ageing of the Cu NMs was found to increase the average particle size and change the composition when compared to pristine Cu and CuO NMs.[7]

Izak-Nau *et al.*[8] investigated whether (and to what extent) changes in silver (Ag) NM properties occur over time and under different storage conditions. Ag NM properties were examined immediately after synthesis and after 1, 3 and 6 months of storage at room temperature in the presence or absence of light and at lower temperature (in a fridge) in the absence of light. The authors found that both storage time/conditions and surface chemistry of Ag NMs influenced the evolution of the NM properties over time, and that the resulting changes in the NMs' physicochemical properties influenced their cytotoxicity. The most influential factors on Ag NM ageing were found to be higher temperature and exposure to daylight. Therefore, a clear and time-resolved understanding of changes in physicochemical characteristics of any metal/metal oxide NMs occurring under different conditions seems to be crucial for the interpretation of their biological effects.[8]

Thwala *et al.*[9] studied the toxicity of silver and zinc oxide NMs to duckweed for a period of 4 days and 14 days. The results showed that the potential risks to aquatic plants of the NMs tested were highly dependent on environmental abiotic parameters. It was concluded that the toxicity of Ag NMs and ZnO NMs was driven both by particulates as well as the dissolved ionic species, and was directly influenced by environmental conditions such as pH and organic matter.[9]

With the exception of these studies, there is a general lack of long term investigations of NM behaviour and most work to date has mainly focused on pristine NMs. NM transformations over time and in different environments currently remain poorly studied and documented.[10] Nowack *et al.*[11] concluded that by studying only the pristine material, the environmental fate of the material cannot be determined. Furthermore, changes in the physicochemical environment can result in engineered NMs that are more (or less) hazardous (or bioavailable) than their pristine counterparts. Thus, it is important to carry out ageing studies in order to understand the transformation mechanism(s) taking place with time in different environmental compartments, and to carry out fate and toxicity studies on aged NM samples also in order to understand the complete fate and behaviour of a NM across its life cycle.

Accelerated ageing is a fast-track ageing process, with the aim of obtaining real ageing results in a shorter time (Hemmerich 1998).[28] Ageing studies are used to establish in a short time the chemical stability or physical durability of a material, in order to estimate or "predict" potential long-term serviceability of material systems under the expected conditions of use. They also facilitate better understanding of the possible chemical reactions involved and the physical consequences of ageing a material.[12] This is achieved by subjecting the material to more severe stresses than normal environmental conditions for a much shorter time. Results may then be correlated with real-time observations.

A simplified protocol for accelerated ageing using temperature was developed following the Arrhenius equation, $k = Ae^{\frac{-E_A}{RT}}$, where k is the rate constant, A is the pre-exponential factor, E_A is the activation energy, R is the gas constant and T is temperature. The rate of a chemical reaction doubles for every 10 °C increase in temperature, resulting in a linear relationship.[13] Nonlinear relationships may, however, arise due to multiple chemical reactions occurring in parallel, *i.e.* complex reactions of second or third order or autocatalytic reactions. It is therefore recognised that thermal ageing can provide important information about transformations with time, but should be carefully evaluated.

It is anticipated that a linear transformation of any NM property as a function of time (or temperature when used as a proxy) is unlikely given such properties are interlinked. However, to date there are no standard testing methods for ageing

or accelerated ageing of NMs. This distinct lack of information spurs the need for investigating ageing of NMs so that any results obtained will contribute towards filling some of the numerous gaps in knowledge that exist, and facilitate the design of more realistic exposure scenarios for NM hazard assessment as well as feeding into the design of safer NMs.

This work aims to study the physical (agglomeration, dissolution, loss of the capping agent) and chemical (oxidation state, core chemistry) changes occurring to a fully characterised library of laboratory synthesised comparable PVP capped NMs (where the NM core is copper oxide, zinc oxide or cerium dioxide) and a commercially available uncoated cerium dioxide NM, upon exposure to various temperatures (25, 45, 65 and 80 °C) for a period of 4 weeks. The observed changes as a function of temperature and experimental time are presented in the context of the Arrhenius equation which links temperature with reaction rates and are interpreted as possible outcomes from a longer ageing process under ambient conditions.

2. Methodology

Cerium nitrate hexahydrate, zinc nitrate hexahydrate, copper nitrate trihydrate, acetone and different chain length (10k, 40k or 360k) polyvinylpyrrolidone (PVP) were all used as received from the supplier (Sigma-Aldrich). Uncapped ceria NMs (showing a size of 4.7 ± 1.4 nm by STEM (Fig. S1†) and a DLS size of 172 nm) were obtained from Promethean Particles Ltd (Nottingham, UK).

10k PVP capped ceria, zinc oxide and copper oxide and 40k and 360k PVP capped ceria were synthesised according to Briffa *et al.*[14] 10k PVP capped metal oxide NMs were *ca.* 5–6 nm, 40k PVP capped NMs were *ca.* 7–8 nm and 360k PVP capped nanoparticles were *ca.* 19–20 nm in diameter. The PVP samples were used as prepared whilst the uncapped samples were prepared by mixing 100 μL of the NM dispersions having an initial concentration of ~2 wt% in water with 4900 μL ultrapure water (UPW, resistivity 18.2 MΩ cm).

The selection of the above NMs was made with the aim to compare the effects of temperature on a series of metal oxide core NMs with 10k PVP capping and a series of different PVP chain length capped ceria NMs representing a range of particle sizes, and the effects on capped *versus* uncapped ceria NMs.

Three replicates of each of the NM dispersions (5 mL) were placed in closed vials on a shaker set at 80 rpm in a Raven 2 incubator. The temperature was set and the ageing was carried out for 28 days. The 4 week duration was chosen since it is a longer time period than that currently presented in the literature and a sufficiently long period to determine the influence of temperature, given that the PVP capped metal oxide NMs were found to be stable at room temperature, when measured by DLS, for a minimum of six months.[14]

The temperature ageing study was carried out at 25, 45, 65 and 80 °C. The first temperature is often used as the reference room temperature and the final one is lower than the boiling point of water to avoid the physical impact of boiling. The other temperatures fall within the range of 25–80 °C in order to effectively cover the chosen range. Using the concept of the Arrhenius link between the temperature and reaction rate, whereby the rate of a chemical reaction doubles for every 10 °C increase in temperature, the experiments simulated ageing equivalent to 4, 16, 64 and 181 weeks (*i.e.* >3.5 years).

Sample characterisation took place for each repeat of each sample at various time points (t = 0, 4, 12, 24, 48, 72, 120, 168, 336, 504, 672 hours) in solution by means of DLS, both sizing and zeta potential, and UV-VIS. TEM imaging and XPS analysis took place on air-dried samples at t = 0 and at the end of the 28 days of ageing.

DLS measurements were performed on a Malvern Zetasizer (Nano ZS) at the University of Birmingham. NM samples dispersed in UPW were analysed. Five consecutive size measurements were carried out at 20 °C and averaged to calculate the mean size. The same instrument was used to obtain the zeta potential values. Three consecutive measurements were collected at 20 °C and averaged to calculate the zeta potential.

UV-VIS absorption was recorded by means of a Jenway 6800 UV/vis spectrophotometer at the University of Birmingham. Spectrum scans were obtained in 10 cm long quartz cuvettes from 800–220 nm.

XPS characterisation was carried out at the Karlsruhe Institute for Technology (KIT) in Germany. Samples were prepared by placing a drop of the NM dispersion on the surface of a silicon wafer, which was allowed to air-dry overnight. XPS measurements were performed using a K-Alpha XPS instrument (ThermoFisher Scientific, East Grinstead, UK). All samples were analysed using a microfocused, monochromated Al Kα X-ray source (400 μm spot size). Two random points were analysed for each of the samples. The K-Alpha charge compensation system was employed during analysis, using electrons of 8 eV energy and low-energy argon ions to prevent any localised charge build-up. Data acquisition and processing using Thermo Avantage software is described elsewhere.[15] The spectra were fitted with one or more Voigt profiles (binding energy uncertainty: ±0.2 eV). The analyser transmission function, Scofield sensitivity factors[16] and effective attenuation lengths (EALs) for photoelectrons were applied for quantification. EALs were calculated using the standard TPP-2M formalism.[17] All spectra were referenced to the C 1s peak (C–C, C–H) at 285.0 eV binding energy, controlled by means of the well-known photoelectron peaks of metallic Cu, Ag, and Au, respectively.

TEM samples were prepared on copper grids by means of the drop method. NM imaging was carried out using a JEOL 1200 TEM at an accelerating voltage of 80 kV, performed at the University of Birmingham.

3. Results and discussion

The results obtained and discussed below indicate changes taking place in all properties investigated, *i.e.* oxidation states, capping efficiency, aggregation and dissolution. We

therefore first describe the physical and chemical transformation observations individually and then combine these into a concept for ageing transformation.

3.1 Size & appearance

The size and physical conformation of the NM dispersions exposed to elevated temperatures for a period of 28 days were monitored by means of DLS and TEM (Table S1 in the ESI†). The general trend for all samples as seen from the DLS results (analysed using the cumulant analysis) is a decrease in the size and intensity of the primary size peak of the NMs and the development of a second peak at a larger size (as seen in Fig. 1 for 40k PVP capped ceria at 25 and 80 °C; all other experiments can be found in the ESI†). As a general observation, the higher the temperature, the more rapidly the changes occur. The decrease in primary size could indicate the dissolution of the NMs or the loss of the PVP capping whilst the development of the second peak indicates agglomeration of the NMs, as seen also from the TEM images (Fig. 1 and ESI†), with the caveat that agglomeration can also occur as a result of drying. Furthermore, at higher temperatures, our results indicate greater agglomeration, evidenced by the secondary DLS peak, and additionally, PVP loss and/or particle dissolution, evidenced by the decrease in the intensity of the first peak. It should be noted that the DLS data of the aged samples are only interpreted qualitatively (*i.e.* to indicate particle aggregation) as any secondary peaks are greatly influenced by the noise of larger particles and the samples become far too polydispersed for reliable size identification.

As the exposure temperature increases, the degree of change of size also increases indicating more rapid agglomeration. The TEM images initially show uniform, spherical, well or relatively well-dispersed particles, agglomerating (at higher temperatures possibly even aggregating) more significantly as the temperature is elevated. Despite a similar trend being noted for all samples, significant differences in terms of the

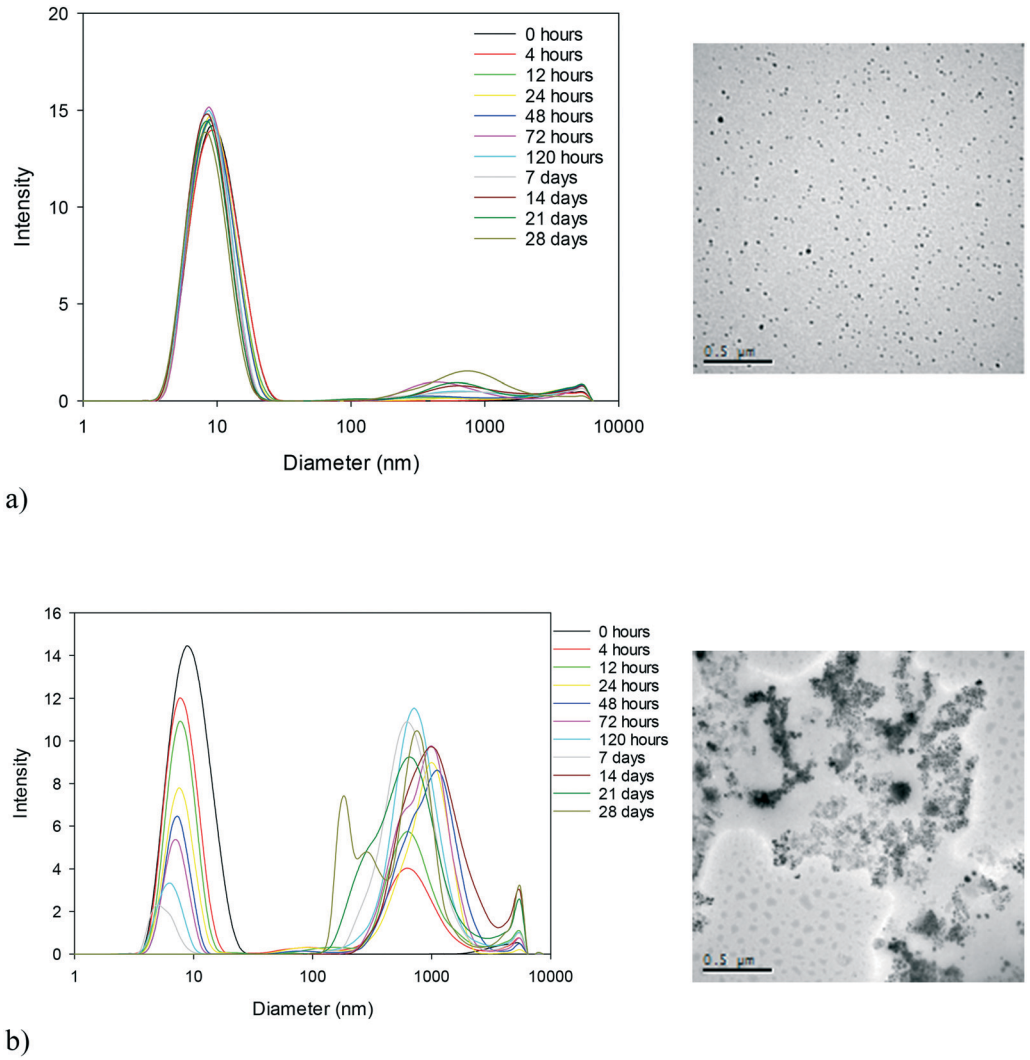

Fig. 1 DLS and TEM results for 40k PVP capped ceria at a) 25 and b) 80 °C.

influence of time (temperature) on the rate of change can be noted between the reference PVP (with no NM present) and capped and uncapped NM samples.

The 10k PVP used as a reference (without a core metal oxide) shows the general trend of a decrease in the intensity of the primary peak size and development of a second peak at a larger size, but the second peak appears only at the 80 °C temperature. This suggests that the PVP itself agglomerates at higher temperatures even in the absence of NMs, and could be indicative of some conformational change or breakdown of the polymer chains allowing agglomeration. The uncapped ceria NMs are the most significantly affected by temperature, particularly at 80 °C. The multitude of DLS peaks, interpreted again qualitatively as indicators of aggregation, and reformed larger aggregated particles observed by TEM seem to indicate that a threshold temperature has been exceeded and the NMs are significantly physically transformed. Such drastic transformations are not observed for the PVP capped NMs, indicating that the PVP influences the behaviour and protects the NMs. In addition, the rate of size change seems to vary for the different NM cores, with the 10k PVP capped ceria NMs indicating the greatest variations followed by the 10k PVP capped copper oxide NMs and then the 10k PVP capped zinc oxide NMs (as shown in Fig. 2). This reveals that the core composition also plays a role in influencing the rate of agglomeration of the NMs during the accelerated ageing process.

3.2 Surface charge

The thermal influence on the surface charge of the samples was measured by means of DLS zeta potential analysis. Prior to analysis the pH of the samples in UPW was measured. All PVP containing samples had a pH of *ca.* 6, whilst the uncapped cerium dioxide NMs had a pH of 7. The change in actual zeta potential values over time can be found in Fig. S2–S8 in the ESI.†

Despite noticeable changes, it is apparent that the temperature does not create a single effect, as it would have been the case if the transformations were first order reactions. Therefore, the observed changes are a result of multiple influencing factors and physical phenomena. Noticeable changes in zeta potential over time for the different temperatures were only observed in the case of the PVP reference samples, the uncapped cerium dioxide NMs and the PVP capped zinc oxide NMs (shown in Fig. 3–5, respectively) indicating that the presence of the capping agent, the capping and core interaction and the core composition are all factors that are affected differently by temperature and all play a role in the measured zeta potential values.

Clearly, of all the NMs, the uncapped ceria NMs' surface charge was influenced the most by temperature (Fig. 4). The fact that the NMs' surface was not protected by a capping agent meant that no steric stabilisation was present to maintain the dispersion and the change in the surface charge is what brings about the agglomeration. The reduced surface charge, and consequently reduced electrostatic repulsion, results in more agglomeration taking place at a faster rate than in the case of the PVP protected samples. The change in zeta potential was most influenced at 80 °C with a significant drop in zeta potential to values very close to 0 mV. The same observation in terms of the most noticeable effect at the highest temperature was observed in both DLS and TEM results.

In the case of PVP capped zinc oxide NMs (Fig. 5) the zeta potential fluctuated over a greater range (from −3 mV to +2.5 mV) than for the other PVP capped samples. Despite this, the values obtained at different temperatures only became significant in relation to one another on the very last measurement taken on day 28.

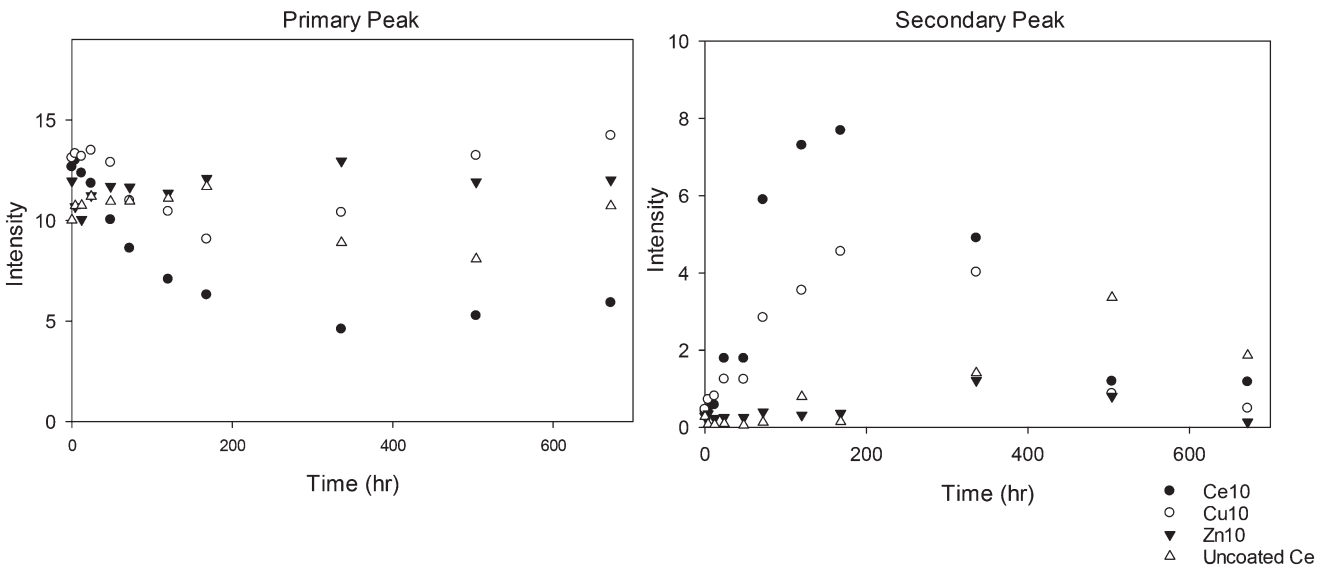

Fig. 2 Intensity *versus* time graphs for 10k PVP capped ceria, zinc oxide, and copper oxide and uncoated ceria NMs at 65 °C showing a trend towards a decrease in the intensity of the DLS primary size peak of the NMs and development of a second peak.

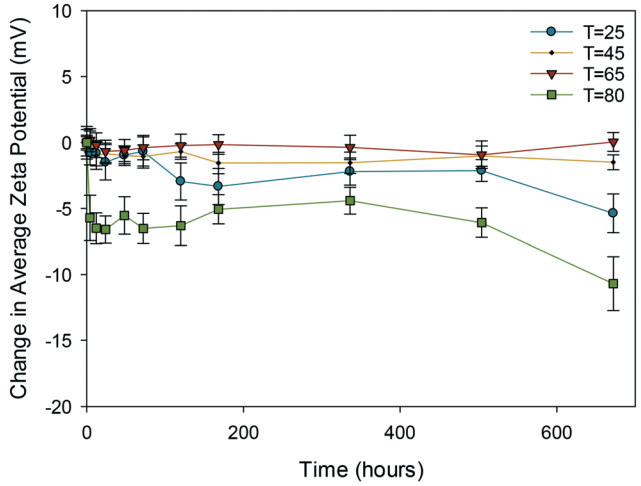

Fig. 3 Change in average zeta potential (mV) as a function of time for 10k PVP reference samples at 25, 45, 65 and 80 °C.

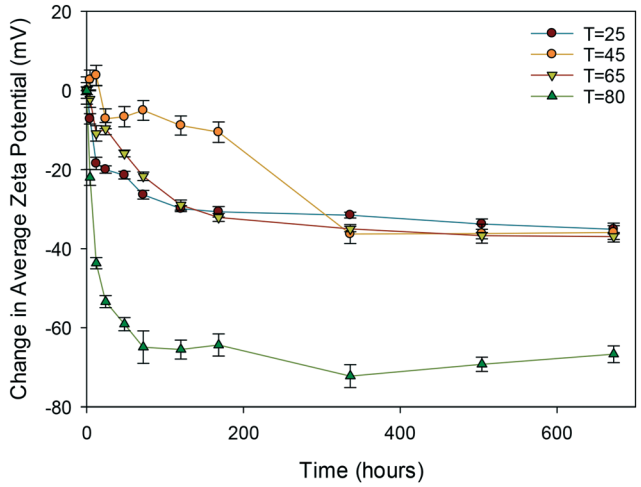

Fig. 4 Change in average zeta potential (mV) as a function of time for the uncapped ceria NMs at 25, 45, 65 and 80 °C.

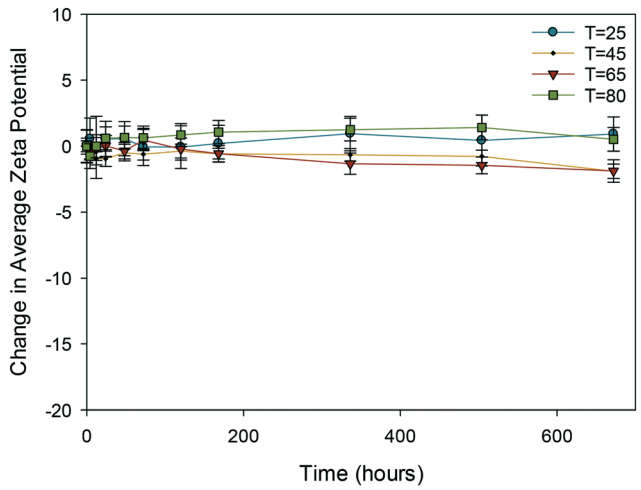

Fig. 5 Change in average zeta potential (mV) as a function of time for 10k PVP capped zinc oxide NMs at 25, 45, 65 and 80 °C.

All the other samples, namely 10k, 40k and 360k PVP capped ceria and 10k PVP capped copper oxide, shown in Fig. S9–S12 in the ESI,† show no significant change in average zeta potential over time, regardless of the exposure temperature. In these cases the average zeta potential values remain similar to the original value, which is around 0 mV due to the PVP steric stabilisation.

3.3 Chemical transformations

3.3.1. X-ray photoelectron spectroscopy (XPS). XPS analysis was carried out to study the influence, if any, of temperature on the oxidation state of the NM surfaces after 28 days. The oxidation state is an important feature to study as it has been suggested that oxidative stress could play an important role in NM toxicity due to the formation of reactive oxygen species (ROS).[18] Thus, knowing the redox states of NMs' over time can suggest whether they become more or less hazardous. Table 1 shows a summary of the oxidation states observed. It should be noted that the PVP chain length affects the redox state of the metal oxide core during synthesis.[14] The 10k PVP reference samples showed no signal indicative of metal oxide as expected.

According to Bêche *et al.*,[19] 2 spin–orbit doublets with Ce $3d_{5/2}$ were fitted at 881.1 and 885.5 as well as Ce $3d_{3/2}$ at 899.4, and 903.7 eV was attributed to Ce^{3+}, whilst Ce^{4+} showed three doublets with Ce $3d_{5/2}$ at 882.7, 888.7 and 898.2, and Ce $3d_{3/2}$ at 901.1, 907.1, and 916.7 eV. The most distinctive feature when observing the XPS spectra of ceria NMs is the presence or absence of a peak at 916.7 eV which is a characteristic satellite peak of Ce^{4+}.[20,21]

The ceria spectra (Fig. S13–S15 in the ESI†) show that the temperature influences the ratio of Ce^{3+} to Ce^{4+} as the peaks change in intensity, particularly that at 916.7 eV. Considering these changes in a quantitative way is non-trivial and a number of studies have discussed alternative approaches for the quantification of ceria oxidation states; these were reviewed by Larachi *et al.*[22] Here, we applied what was deemed the most appropriate approach, *i.e.* consideration of the complete area of the 2 Ce^{3+} doublets and the 3 Ce^{4+} doublets, which were followed and corrected with the corresponding Scofield factors in order to quantify the contribution of each oxidation state.

The 10k PVP capped ceria NMs start off as a mix of Ce^{3+} (~40%) and Ce^{4+} (~60%). The content of Ce^{4+} increases up to 66% at 25 °C and decreases clearly then at 45 °C to 51% and 57% at 65 °C. At 80 °C the sample is clearly

Table 1 Oxidation state recorded by means of XPS

Sample	25 °C	45 °C	65 °C	80 °C
10k Ce	Ce(III), Ce(IV)	Ce(III), Ce(IV)	Ce(III), Ce(IV)	Ce(III)
40k Ce	Ce(III)	Ce(III)	Ce(III)	Ce(III), Ce(IV)
360k Ce	Ce(III)	Ce(III)	Ce(III), Ce(IV)	No signal
Uncapped Ce	Ce(III), Ce(IV)	Ce(III), Ce(IV)	Ce(III), Ce(IV)	Ce(III), Ce(IV)
10k Zn	Zn(II)	Zn(II)	Zn(II)	Zn(II)
10k Cu	Cu(I), Cu(II)	Cu(I), Cu(II)	Cu(I), Cu(II)	Cu(II)

reduced and the presence of Ce^{4+} is no longer detectable. The 40k PVP capped ceria NMs reveal solely Ce(III) up to 80 °C where the NMs are oxidised and the sample shows a small amount of Ce(IV). The 360k PVP capped ceria NMs showed an oxidation at 60 °C and no signal after exposure to 80 °C. The latter may be due to complete dissolution of the NMs at such an elevated temperature and length of exposure. Further support for this conclusion comes from what was originally considered the primary DLS peak, which is nearly non-existent after 28 days, as seen in Table S1.†

The XPS spectra of the uncapped ceria NMs reveal the presence of Ce^{3+} and Ce^{4+}, with the main oxidation state of the NMs being 4+, and also show minimal changes over time at all temperatures studied (Fig. S16 in the ESI†). The lack of the PVP capping, which acts as a reducing agent, is probably the reason why the uncoated NMs are not as easily reduced as the PVP capped metal oxide NMs described next.

All copper spectra show the presence of strong satellite peaks at about 943 eV, indicating the presence of Cu(II).[23,24] The 10k PVP capped copper oxide NMs show two peaks up to 65 °C, one at 932.5 and the other at 934.5 eV, indicating that both copper(I) and copper(II) species are present. At 80 °C any Cu(I) present has been completely oxidised to Cu(II). PVP capped zinc oxide NMs show the presence of Zn(II) only and no significant changes, implying that they are unaffected by temperature even over long times.

To conclude, redox transformations were very important for ceria and, to a lesser extent copper oxide but not for zinc oxide, demonstrating the importance of core chemistry on the ageing process. Furthermore, changes in the core metal oxidation state of the PVP capped ceria NMs show that even though capping stabilises the NM dispersions, the cores are not protected from external influences such as temperature changes.

3.3.2. UV-VIS. UV-VIS analysis revealed information about both the chemical and physical properties of the NMs as well as information about the changes affected by temperature.

In all samples where PVP is present, whether with or without a NM core, a peak just below 450 nm could be seen which is due to PVP oxidation products, as seen in the literature.[25] A general observation from the UV-VIS data is that the spectral signal recorded was much weaker at the end of the 28 day period than at the start of the experiment. The UV-VIS data therefore clearly show transformations of the NMs taking place over time possibly indicating agglomeration and sedimentation of the NMs and therefore lower (or variable) signals due to sampling heterogeneity. Although according to Beer–Lambert's law absorbance can be directly related to concentration, this only applies when the path length and extinction coefficient are unchanged, which is not the case under the experimental conditions of this study. With reference to the location of the peaks, it should be noted that small shifts of UV-VIS peaks are possible due to particle interactions with other components in the media such as the PVP. Furthermore, the 10k PVP reference samples showed no signal indicative of metal oxide as expected.

The rate at which these transformations occur seemed to be influenced by temperature. The decrease in UV-VIS signal intensity is notable for the 10k PVP reference samples (Fig. S19†), demonstrating that some of the transformations would have resulted from the degradation and/or dissociation of the capping from the NMs. The PVP degradation eventually exposes the metal core, and the onset of this transformation is recorded in Table 2. This was demonstrated in a side study (Fig. S26†) whereby increasing the amount of PVP added to the uncapped ceria NP dispersion ended up shielding the metal oxide absorption peak making it less distinguishable.

In the case of the ceria samples, peaks were identified at 254 nm and 300 nm for Ce^{3+} and Ce^{4+}, respectively.[14,26,27] In the case of the zinc oxide, two peaks were found at 250 nm and just below 300 nm, which were representative of PVP and zinc oxide, respectively. Since a similar behaviour to that seen for the PVP capped ceria NMs is observed, this suggests that the PVP capping in fact becomes less effective with elevated temperature. In the spectra of the 10k PVP capped copper oxide NMs peaks at 280 nm and 440 nm are noticeable which are characteristic of CuO and Cu_2O, respectively.

The uncapped ceria NM spectra show a single peak with a maximum intensity at 300 nm. This corresponds to Ce^{4+} as also determined from the XPS results. These UV-VIS spectra show no change in the peak position, indicating that this ceria NMs' initial oxidation state is unchanged over 28 days as seen from XPS. The spectra imply the same oxidation state at the start and end of the experiment, though intermediate transformations could have occurred when no measurements were taken. The only variation noted is a decrease in intensity over time (indicating a loss of nanoscale features), the extent of which seems to be influenced by temperature.

3.4 Transformation behaviour

It is desirable to interpret the above observations in the context of the Arrhenius equation, in order to, at least qualitatively,

Table 2 Time point in hours at which the metal oxide peak becomes apparent in the UV-VIS spectra

Sample	25 °C	45 °C	65 °C	80 °C
10k Ce	0	24	504	Not observed
40k Ce	Invisible due to PVP	Invisible due to PVP	24	336
360k Ce	Invisible due to PVP	0 hours	504	336
Uncapped Ce	N/A	N/A	N/A	N/A
10k Zn	Invisible due to PVP	48	336	Not observed
10k Cu	Invisible due to PVP	48	120	120

allow correlation between time (or temperature) and the changes in any one of the four properties considered here. To enable such a pattern to emerge, we interpreted our results as follows: where an apparent linear trend transformation occurred, this was interpreted as a change in a single property. For example, if a continuous size increase was observed, this indicated an aggregation-only (or aggregation-dominated) transformation regime, whereas if a continuous size decrease was observed, this indicated a dissolution-only (or dissolution-dominated) transformation. Redox transformations progressed independently of other changes, whereas changes in capping efficiency influenced both aggregation and dissolution and therefore resulted in an overall non-linear effect.

In order to rationalise the range of transformations, we recorded the point at which each experiment showed a deviation in the trend of the observed transformation and considered this as the onset of complex behaviour. Whilst indicating an apparent linear trend, we considered the process to show a single transformation. These observations enabled a qualitative assessment of relative rates of transformation as follows: aggregation (size increase, DLS data) is the fastest transformation, followed by dissolution (size decrease, DLS data) and finally loss of capping stability (multiple changes, DLS and UV-VIS data) which is the slowest process. Redox changes are driven towards an increase in oxidation state, although no rate estimate can be made from our data.

We have summarised the overall behaviour in Fig. 6, using as an example the case of 40k PVP capped ceria, where a relatively long-lasting apparently linear trend was recorded in the observed transformations and where, for that apparently linear part, we considered temperature as a proxy for time. It should be noted that in most experiments multiple changes were recorded in parallel and therefore the net effect was chaotic early on in the process, suggesting transformations occurring irreversibly and competitively (*i.e.* dissolution *versus* aggregation *versus* loss of capping).

Fig. 6 Schematic depicting change in NM properties as a function of temperature, as a proxy for time for 40k PVP capped ceria as an example. The arrows show the direction of change for each property, specifically: from a lower to higher oxidation state, from a disaggregated to aggregated state, from larger to smaller individual particles due to dissolution and from the capped to uncapped state. Though not always the case for all samples, in this case the transformations occur in a linear fashion and the rate varies (as shown by the gradient in the slope of individual arrows).

4. Conclusions

Studying the behaviour of NMs in different environments reveals important information that can influence NM' toxicity. This work allowed for the study of thermal transformations of NMs, revealing significant characteristic physical and chemical property behaviours of PVP capped metal oxide NMs and an uncapped ceria NM. This thermal treatment was implemented as a possible proxy for ageing of NMs in order to enable prediction of longer term transformations that would be experimentally unfeasible to test.

These findings reveal two phases of interest in a NMs' life cycle. These are their effects over a short time period in different temperature environments and the estimated or predicted potential long-term behaviour. The latter is revealed through the studies at elevated temperature, speeding up the processes taking place and therefore allowing temperature to be a qualitative proxy for time. The Arrhenius equation, which links temperature with reaction rates, is the guiding principle of the work presented here. It is shown that transformations are accelerated by temperature, as by time, although the process of ageing involves several transformations occurring simultaneously and therefore the net effect is nonlinear and cannot be used in a quantitative manner. Although as yet we cannot directly link the accelerated ageing testing with real-life studies due to the lack of real prolonged environmental ageing data, this study shows the types of environmental changes that are likely to occur and demonstrates that, in fact, it is not the pristine NMs that are present in the environment but the ones that may have been transformed physically and chemically by interaction with biomolecules and organisms in the environment. This highlights the importance of carrying out toxicity and behavioural studies on aged NMs as well as the pristine ones in order to fully understand their behaviour in the environment. Furthermore, the data presented here emphasise the complex features influencing the life-cycle of NMs, and that numerous physical and chemical changes may occur in parallel or sequentially, as well as the need for further studies of this nature to be carried out.

Results showed that the NM behaviour was influenced by both particle specific variables, including core composition, capping and core interaction and capping molecule size, and external factors, in this case temperature as a proxy for time. They further showed that any surface modification, especially found on redox sensitive NMs, may have a complex role in their stability, both in terms of the level of protection from interactions with the environment and also in terms of influencing their longer term redox state.

DLS and TEM revealed a general trend involving a decrease in the primary size of the NMs and, in the case of DLS, the development of a second peak at a larger size indicating agglomeration as seen also by TEM, as a function of temperature and time. Differences in these changes and the rate of change were revealed amongst the PVP used as a reference and capped and uncapped samples. 10k PVP capped ceria had the highest rate of size change followed by 10k PVP capped copper oxide, whereas 10k PVP capped zinc oxide had the smallest rate, revealing that the core composition also plays a role in influencing the rate of agglomeration. Furthermore, it is important to note that the presence of PVP does not inhibit agglomeration beyond a certain time point. The uncapped ceria sample seemed to have a threshold temperature of 80 °C, beyond which the particles' size and aggregation were significantly increased.

The surface charge of all the capped particles shows very little change as a function of time regardless of the temperature, as indicated by the zeta potential measurements. The PVP samples used for reference showed some slight changes. However, due to the lack of shielding from the media, the most significant changes were noted for the uncapped ceria, particularly at 80 °C. This highlights the complex role of the surface modification and its own longevity and stability, in terms of the environmental influence on the NMs.

Chemical analysis, studied by XPS and UV-VIS, confirmed metal core oxidation states and indicated changes in the oxidation state, NM dissolution and loss of capping. The core composition valence state, therefore, is an important feature that could influence dissolution and toxicity. Changes in the valence state were impacted by temperature, core chemistry and/or PVP reducing ability on the core.

Furthermore, UV-VIS indicated the probability of dissolution, agglomeration and possibly other transformations of the NMs and PVP, due to a decrease in peak intensity over the 28 day period and the development of a second peak corresponding to the core metal. The extent of change was influenced by temperature and increased with increasing temperature.

The PVP capping, despite stabilising the NMs, still allowed the NMs to undergo physical and chemical changes, though in many cases to a lesser extent than the equivalent uncapped NMs. Additionally, the capping appeared less effective as a function of time and temperature. This was evidenced by the presence of NM and PVP agglomeration observed by DLS and TEM as well as through UV-VIS where the metal peak was originally shadowed by the PVP peak but at higher temperatures became noticeable, particularly in the case of the cerium dioxide NMs.

This study shed light on the complexity of NM ageing with multiple changes occurring simultaneously. Such complexity makes it difficult to isolate a single transformation and simply measure it using a single analytical technique. Furthermore, it showed how specific NM behaviour can be affected by the full spectrum of NM properties, both physical and chemical, the environment, and the interaction between these variables. In this study, core composition, capping agent molecular weight, capping and core interaction, the presence or absence of capping, and NM size all influenced the particle ageing behaviour. Moreover, in spite of the PVP capping stabilising the NM dispersions, it did not fully protect them from external factors, perhaps due to the PVP shell being typically hydrated and thus the metal oxide surface being accessible to ions, electrons, and biomolecules.

Conflicts of interest

There are no conflicts to declare.

Acknowledgements

The authors acknowledge financial support from the FP7 funded project NanoMILE (Grant Agreement no. 310451 to EVJ, IL, SMB) and the Endeavour Scholarship Scheme (Group B) (to SMB). Thoughtful reviews by two referees and editorial handling by Professor Greg Lowry enabled the authors to substantially improve the quality of the manuscript.

References

1 V. Sarathy, *et al.*, Aging of Iron Nanoparticles in Aqueous Solution: Effects on Structure and Reactivity, *J. Phys. Chem. C*, 2008, **112**(7), 2286–2293.
2 D. Mitrano, *et al.*, *Report on environmental transformation reactions*, 2014.
3 E. Valsami-Jones and I. Lynch, How safe are nanomaterials?, *Science*, 2015, **350**(6259), 388–389.
4 I. Lynch, *et al.*, Strategy for Identification of Nanomaterials' Critical Properties Linked to Biological Impacts: Interlinking of Experimental and Computational Approaches, in *Advances in QSAR Modeling: Applications in Pharmaceutical, Chemical, Food, Agricultural and Environmental Sciences*, ed. K. Roy, Springer International Publishing, Cham, 2017, pp. 385–424.
5 C. Botta, *et al.*, TiO2-based nanoparticles released in water from commercialized sunscreens in a life-cycle perspective: Structures and quantities, *Environ. Pollut.*, 2011, **159**(6), 1543–1550.
6 S. V. N. T. Kuchibhatla, *et al.*, Influence of aging on the properties of cerium oxide nanoparticles - implications to quantum confinement effect, in *Nanotechnology (IEEE-NANO), 2011 11th IEEE Conference on*, 2011.
7 I. A. Mudunkotuwa, J. M. Pettibone and V. H. Grassian, Environmental Implications of Nanoparticle Aging in the Processing and Fate of Copper-Based Nanomaterials, *Environ. Sci. Technol.*, 2012, **46**(13), 7001–7010.
8 E. Izak-Nau, *et al.*, Impact of storage conditions and storage time on silver nanoparticles' physicochemical properties and implications for their biological effects, *RSC Adv.*, 2015, **5**(102), 84172–84185.
9 M. Thwala, *et al.*, The oxidative toxicity of Ag and ZnO nanoparticles towards the aquatic plant Spirodela punctuta and the role of testing media parameters, *Environ. Sci.: Processes Impacts*, 2013, **15**(10), 1830–1843.

10 G. V. Lowry, *et al.*, Transformations of Nanomaterials in the Environment, *Environ. Sci. Technol.*, 2012, **46**(13), 6893–6899.
11 B. Nowack, *et al.*, Potential scenarios for nanomaterial release and subsequent alteration in the environment, *Environ. Toxicol. Chem.*, 2012, **31**(1), 50–59.
12 R. L. Feller, *Accelerated Aging: Photochemical and Thermal Aspects*, Getty Conservation Institute, 1995.
13 J. Clarke, *Rate Constants and the Arrhenius Equation*, 2002, Available from: http://www.chemguide.co.uk/physical/basicrates/arrhenius.html.
14 S. M. Briffa, *et al.*, Development of scalable and versatile nanomaterial libraries for nanosafety studies: polyvinylpyrrolidone (PVP) capped metal oxide nanoparticles, *RSC Adv.*, 2017, **7**(7), 3894–3906.
15 K. L. Parry, *et al.*, *ARXPS characterisation of plasma polymerised surface chemical gradients*, ed. M. R. Alexander, Chichester, UK, 2006, pp. 1497–1504.
16 J. H. Scofield, Hartree-Slater subshell photoionization cross-sections at 1254 and 1487 eV, *J. Electron Spectrosc. Relat. Phenom.*, 1976, **8**(2), 129–137.
17 S. Tanuma, C. J. Powell and D. R. Penn, Calculations of electron inelastic mean free paths. V. Data for 14 organic compounds over the 50–2000 eV range, *Surf. Interface Anal.*, 1994, **21**(3), 165–176.
18 A. Aydin, H. Sipahi and M. Charehsaz, Nanoparticles Toxicity and Their Routes of Exposures, in *Recent Advances in Novel Drug Carrier Systems*, 2012.
19 E. Bêche, *et al.*, Ce 3d XPS investigation of cerium oxides and mixed cerium oxide (CexTiyOz), *Surf. Interface Anal.*, 2008, **40**(3–4), 264–267.
20 E. G. Heckert, *et al.*, The role of cerium redox state in the SOD mimetic activity of nanoceria, *Biomaterials*, 2008, **29**(18), 2705–2709.
21 P. W. Park and J. S. Ledford, Effect of Crystallinity on the Photoreduction of Cerium Oxide: A Study of CeO2 and Ce/Al2O3 Catalysts, *Langmuir*, 1996, **12**(7), 1794–1799.
22 F. ç. Larachi, *et al.*, Ce 3d XPS study of composite CexMn1−xO2−y wet oxidation catalysts, *Appl. Surf. Sci.*, 2002, **195**(1), 236–250.
23 M. C. Biesinger, *et al.*, Resolving surface chemical states in XPS analysis of first row transition metals, oxides and hydroxides: Cr, Mn, Fe, Co and Ni, *Appl. Surf. Sci.*, 2011, **257**(7), 2717–2730.
24 I. Platzman, *et al.*, Oxidation of Polycrystalline Copper Thin Films at Ambient Conditions, *J. Phys. Chem. C*, 2008, **112**(4), 1101–1108.
25 C. E. Hoppe, *et al.*, One-Step Synthesis of Gold and Silver Hydrosols Using Poly(N-vinyl-2-pyrrolidone) as a Reducing Agent, *Langmuir*, 2006, **22**(16), 7027–7034.
26 T. Herrling, M. Seifert and K. Jung, Cerium Dioxide: Future UV-filter in Sunscreen?, *SOFW J.*, 2013, **139**(5), 10–15.
27 S. Tsunekawa, T. Fukuda and A. Kasuya, Blue shift in ultraviolet absorption spectra of monodisperse CeO2−x nanoparticles, *J. Appl. Phys.*, 2000, **87**(3), 1318–1321.
28 K. J. Hemmerich, *General Aging Theory and Simplified Protocol for Accelerated Aging of Medical Devices [Homepage of Medical Device and Diagnostic Industry]*, 1998, [Online], 1st July 1998-last update, Available: http://www.mddionline.com/article/general-aging-theory-and-simplified-protocol-accelerated-aging-medical-devices [2016, 10/20].